MODELLING OF A CASCADE VAPOUR COMPRESSION CYCLE EMPLOYING BRAZED PLATE HEAT EXCHANGERS

Enio Pedone Bandarra Filho – bandarra@ufu.br
Frank Wiliam Adolfo Blanco Ojeda - frank_blanco@ufu.br
Faculdade de Engenharia Mecânica – Universidade Federal de Uberlândia
José Alberto Reis Parise – Parise@puc-rio.br
Departamento de Engenharia Mecânica – Pontifícia Universidade Católica do Rio de Janeiro.

R4 – Special and industrial application

Abstract. *A simulation model was developed to study the steady-state operation of a cascade vapour compression refrigeration system. Given the dependence of the heat transfer and pressure drop mechanisms on local governing conditions on each side of the brazed plate heat exchangers, a multi-zone approach was adopted. Accordingly, each heat exchanger was divided into a number of control volumes for which mass and energy conservation, heat transfer rate and effectiveness equations were applied. Appropriate correlations were chosen for the zone averaged heat transfer and pressure drop coefficients, for single phase, condensing or evaporating flows. The resulting model (system of non-linear algebraic equations) was numerically solved to study the effect on system performance and heat exchanger areas of the following: (i) refrigerant pairs (among R717, R407C, R404A, R744 and R410A); (ii) cascade-condenser approach (condensing to evaporating temperature differential); and (iii) mass flux per heat exchanger channel.*

Keywords: *Cascade refrigeration, Brazed plate heat exchanger, Moving boundary method, Simulation, Cascade-condenser.*

1. INTRODUCTION

Cascade refrigeration systems come into play for low temperature applications when a single-stage vapour compression refrigeration cycle may prove insufficient for the task (Lee et al., 2006). They have been the focus of interest for more than a decade (e.g., Pearson, 1999; Sawalha, 2005), as reported by Bansal and Jain (2007). Cascade refrigeration cycles widen the possibilities for low-temperature refrigeration systems running on refrigerants with lower environmental impact (zero ODP and very low GWP) and with adequate pressures at both heat sink (ambient) and heat source (refrigerated medium) temperatures. In this respect, two experimental works, both dealing with a pair of natural refrigerants, NH3-CO2, have been recently reported in the literature (Bingming et al., 2009; Dopazo and Fernández-Seara, 2011). Analytical studies can also be found, most of them presenting some kind of optimization: thermoeconomic (Rezayan and Behbahaninia, 2011), of allocation of heat exchanger inventory (Bhattacharyya et al., 2008) and of the intermediate condensing/evaporating temperatures (Lee et al., 2006; Getu and Bansal, 2008; Dopazo et al., 2009; Di Nicola et al., 2011; Messineo and Panno, 2011a, 2011b). An exergy analysis is also reported (Kilicarslan and Hosoz, 2010).

As the low temperature refrigerant in a cascade system, the CO2 has good thermodynamic properties, very low GWP and operates below the critical temperature. Concerning the high-temperature stage, a safer utilization of environmentally benign refrigerants that may present toxicity or flammability issues, like ammonia, is made possible by means of system confinement (to the machine room) and reduction of the refrigerant charge. Further on the direct impact of refrigeration systems (leakage of the refrigerant inventory), Poggi et al. (2008) have shown that brazed-plate evaporators and condensers may contribute to a significant reduction on refrigerant charge, if compared to more conventional heat exchangers, in particular those with refrigerant flowing outside tubes. The technologies of the cascade refrigeration cycle and the brazed-plate heat exchangers can thus be combined to provide low-temperature refrigeration systems with reduced environmental impact. The present paper is concerned with the development of a simulation model for a two-circuit cascade-refrigeration system, Fig. 1. In particular, evaporator, cascade-condenser and condenser of the brazed-plate type were studied.

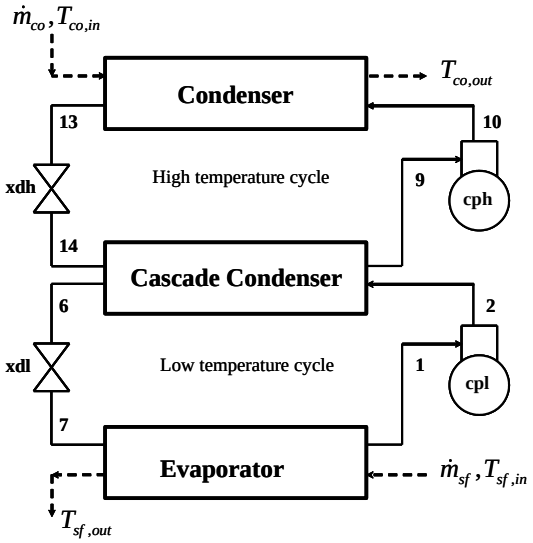

Figure 1 Cascade refrigeration system with two vapour compression cycles.

2. MATHEMATICAL MODEL

The mathematical model is outlined below, starting with the definition of the control volumes, followed by the modeling of each component. By means of the multi-zone (or moving boundary) method (for example, Le et al., 2004), each of the three heat exchangers was divided into a number of control volumes (the evaporator in two, the cascade-condenser in four and the condenser in three), to cope with the distinct heat transfer characteristics that occur within them (boiling or condensation, liquid or gas single-phase heat transfer).

2.1 Control volumes

Thirteen control volumes comprise the cascade vapour compression refrigeration cycle, Fig. 2. They are: the evaporator (EV) zones, boiling (bo) and superheating (sh), low-temperature compressor (cpl) and expansion device (xdl), the cascade-condenser (CC) four distinct zones (I - subcooling to boiling; II – condensing to boiling; III – desuperheating to boiling; IV – desuperheating to superheating), high-temperature compressor (cph) and expansion device (xdh), and the condenser (CD) desuperheating (ds), condensing (cs) and subcooling (sc) zones. The cascade-condenser was divided in that manner so that each of its zones would have one single heat transfer condition, i.e., single or two-phase heat transfer in either side. The division depicted in Fig. 2, with the high temperature cycle boiling refrigerant meeting all the desuperheating, condensing and subcoling stages of the low temperature cycle refrigerant, is not the only one possible for the cascade-condenser, though it was chosen for being the most probable to happen under typical operating conditions.

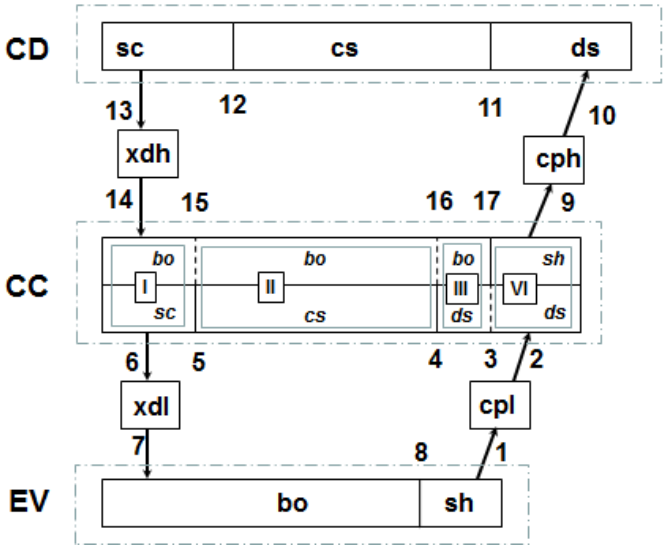

Figure 2 System components, control volumes and refrigerant states for the mathematical model, with low temperature (1-2-3-4-5-6-7-8) and high temperature (9-10-11-12-13-14-15-16-17) circuits.

2.2 Compressors

A simple efficiency-based model is employed for the compressors. The isentropic and volumetric efficiencies are related to compressors suction and discharge thermodynamic states, as well as to the refrigerant mass flow rates, as follows:

$$\eta_{s,cpl} = \frac{\left(h_{2s} - h_1\right)}{\left(h_2 - h_1\right)} \tag{1}$$

$$\eta_{s,cph} = \frac{\left(h_{10s} - h_9\right)}{\left(h_{10} - h_9\right)} \tag{2}$$

$$s_{2s} = s_1 \tag{3}$$

$$s_{10s} = s_9 \tag{4}$$

$$\eta_{v,cpl} = \frac{v_1 \dot{m}_{rl}}{\dot{V}_{cp,LTC}} \tag{5}$$

$$\eta_{v,cph} = \frac{v_9 \dot{m}_{rh}}{\dot{V}_{cp,HTC}} \tag{6}$$

Polynomial correlations, as suggested by Brown et al. (2002) and Lee et al. (2006), were employed for the isentropic efficiency, allowing for the determination of the adiabatic compressor power consumption, as follows:

$$\eta_{s,cp} = \sum_{i=1}^{3}\left(b_i R_p^i\right) \tag{7}$$

$$\dot{W}_{cpl} = \dot{m}_{rl}\left(h_2 - h_1\right) \tag{8}$$

$$\dot{W}_{cph} = \dot{m}_{rh}\left(h_{10} - h_9\right) \tag{9}$$

2.3 Condenser

Each zone of the condenser is treated as an independent heat exchanger, with its own set of equations (Martins Costa and Parise, 1993; Bansal and Purkayastha, 1998). Overall counter-flow is assumed. Equations (10) to (20) describe the gas-to-liquid and liquid-to-liquid single-phase heat exchange in the desuperheating (ds) and subcooling (sc) zones. They represent the refrigerant and cooling fluid energy balance equations, as well as the heat transfer rate:

$$\dot{Q}_{ds} = \dot{m}_{rh}\left(h_{10} - h_{11}\right) \tag{10}$$

$$\dot{Q}_{ds} = \dot{m}_{co}\, c_{p,co}\left(T_{co,out} - T_{co,b}\right) \tag{11}$$

$$\dot{Q}_{ds} = C_{\min,ds}\, \varepsilon_{ds}\left(T_{10} - T_{co,b}\right) \tag{12}$$

$$\dot{Q}_{sc} = \dot{m}_{rh}\left(h_{12} - h_{13}\right) \tag{13}$$

$$\dot{Q}_{sc} = \dot{m}_{co}\, c_{p,co}\left(T_{co,a} - T_{co,in}\right) \tag{14}$$

$$\dot{Q}_{sc} = C_{\min,sc}\, \varepsilon_{sc}\left(T_{12} - T_{co,in}\right) \tag{15}$$

Where

$$C_{\min,ds} = \min\left(\dot{m}_{co} c_{p,co}; \dot{m}_{rh} c_{p,v,ds}\right) \tag{16}$$

And

$$C_{\min,sc} = \min\left(\dot{m}_{co} c_{p,co}; \dot{m}_{rh} c_{p,l,sc}\right) \tag{17}$$

The effectiveness for these two zones (counter-flow single-phase heat transfer) is:

$$\varepsilon = \frac{1-\exp\left[-NTU\left(1-C^*\right)\right]}{1-C^*\exp\left[-NTU\left(1-C^*\right)\right]} \text{ , if } C^* \neq 1 \text{ or } \varepsilon = \frac{NTU}{NTU+1}, \text{ if } C^* = 1 \quad (18)$$

Where

$$C^* = \frac{C_{\min}}{C_{\max}} \quad (19)$$

$$NTU = \frac{U\,A}{C_{\min}} \quad (20)$$

For the condensing zone, the following equations apply:

$$\dot{Q}_{cs} = \dot{m}_{rh}\left(h_{11} - h_{12}\right) \quad (21)$$

$$\dot{Q}_{cs} = \dot{m}_{co}\,c_{p,co}\left(T_{co,b} - T_{co,a}\right) \quad (22)$$

$$\dot{Q}_{cs} = \dot{m}_{co}\,c_{p,co}\varepsilon_{cs}\left(T_{11} - T_{co,a}\right) \quad (23)$$

For pure refrigerants and azeotropic mixtures, the condensing zone effectiveness is:

$$\varepsilon_{cs} = 1-\exp\left(-\frac{U_{cs}\,A_{cs}}{\dot{m}_{co}\,c_{p,co}}\right) \quad (24)$$

The condenser total power output and total heat transfer area are, respectively:

$$\dot{Q}_{cd} = \dot{Q}_{ds} + \dot{Q}_{cs} + \dot{Q}_{sc} \quad (25)$$

$$A_{cd} = A_{ds} + A_{cs} + A_{sc} \quad (26)$$

Finally, the prescribed condenser outlet degree of subcooling provides:

$$\Delta T_{sc,HTC} = T_{12} - T_{13} \quad (27)$$

2.4 Expansion devices

It is assumed that both devices are thermostatic expansion valves which provide constant superheat at the outlet of the evaporator and at the outlet of the cascade-condenser on the high temperature cycle side (its corresponding evaporator).

$$T_1 = T_8 + \Delta T_{sh,LTC} \quad (28)$$

$$T_9 = T_{17} + \Delta T_{sh,HTC} \quad (29)$$

Given that there is no work done and neglecting the heat transfer from the environment, from the energy conservation equation, the expansion process is isenthalpic.

$$h_6 = h_7 \quad (30)$$

$$h_{13} = h_{14} \quad (31)$$

2.5 Evaporator

The evaporator is treated similarly to the condenser. Two control volumes, are established, dictated by the phase change of the refrigerant: boiling and superheating zones. The energy balances, heat transfer rate and effectiveness equations for boiling and superheating zones, respectively, are:

$$\dot{Q}_{bo} = \dot{m}_{rl}\left(h_8 - h_7\right) \tag{32}$$

$$\dot{Q}_{bo} = \dot{m}_{sf}\, c_{p,sf}\left(T_{sf,m} - T_{sf,out}\right) \tag{33}$$

$$\dot{Q}_{bo} = \dot{m}_{sf}\, c_{p,sf}\, \varepsilon_{bo}\left(T_{sf,m} - T_7\right) \tag{34}$$

$$\dot{Q}_{sh} = \dot{m}_{rl}\left(h_1 - h_8\right) \tag{35}$$

$$\dot{Q}_{sh} = \dot{m}_{sf}\, c_{p,sf}\left(T_{sf,in} - T_{sf,m}\right) \tag{36}$$

$$\dot{Q}_{sh} = C_{\min,sh}\, \varepsilon_{sh}\left(T_{sf,m} - T_8\right) \tag{37}$$

Similarly, to the condenser, counter-flow effectiveness equations, like (18) to (20), also apply to the superheating zone. For pure refrigerants and azeotropic mixtures, the boiling zone effectiveness is:

$$\varepsilon_{bo} = 1 - \exp\left(-\frac{U_{bo}\, A_{bo}}{\dot{m}_{sf}\, c_{p,sf}}\right) \tag{38}$$

The total refrigeration capacity and evaporator total heat transfer area are, respectively:

$$\dot{Q}_{ev} = \dot{Q}_{bo} + \dot{Q}_{sh} \tag{39}$$

$$A_{ev} = A_{bo} + A_{sh} \tag{40}$$

2.6 Cascade-condenser

Energy balances and heat transfer rate equations, for each of the control volumes, are presented below.

2.6.1 Control volume I - subcooling to boiling:

$$\dot{Q}_I = \dot{m}_{rh}\left(h_{15} - h_{14}\right) \tag{41}$$

$$\dot{Q}_I = \dot{m}_{rl}\left(h_5 - h_6\right) \tag{42}$$

$$\dot{Q}_I = C_{\min,I}\, \varepsilon_I \left(T_5 - T_{14}\right) \tag{43}$$

2.6.2 Control volume II – condensing to boiling:

$$\dot{Q}_{II} = \dot{m}_{rh}\left(h_{16} - h_{15}\right) \tag{44}$$

$$\dot{Q}_{II} = \dot{m}_{rl}\left(h_4 - h_5\right) \tag{45}$$

$$\dot{Q}_{II} = \begin{cases} U_{II}\, A_{II}\left(T_4 - T_{15}\right) & : \text{no temperature glide} \\ C_{\min,II}\, \varepsilon_{II}\left(T_4 - T_{15}\right) & : \text{with temperature glide} \end{cases} \tag{46}$$

2.6.3 Control volume III – desuperheating to boiling:

$$\dot{Q}_{III} = \dot{m}_{rh}\left(h_{17} - h_{16}\right) \tag{47}$$

$$\dot{Q}_{III} = \dot{m}_{rl}\left(h_3 - h_4\right) \tag{48}$$

$$\dot{Q}_{III} = C_{\min,III}\, \varepsilon_{III}\left(T_3 - T_{16}\right) \tag{49}$$

2.6.4 Control volume IV – desuperheating to superheating:

$$\dot{Q}_{IV} = \dot{m}_{rh}\left(h_9 - h_{17}\right) \tag{50}$$

$$\dot{Q}_{IV} = \dot{m}_{rl}\left(h_2 - h_3\right) \tag{51}$$

$$\dot{Q}_{IV} = C_{\min,IV}\, \varepsilon_{IV}\left(T_2 - T_{17}\right) \tag{52}$$

For refrigerants with no temperature glide, equations (18) to (20) apply for the effectivenesses of zones I and IV (single-phase to single-phase), and an equation equivalent to (38), for zone III (heat transfer between single-phase and boiling

fluids). When significant temperature glide exists, equations (22) to (24), together with the corresponding two-phase average specific heat, , apply for all four control volumes.

Finally, in a similar way to the condenser and evaporator:

$$\dot{Q}_{cc} = \dot{Q}_I + \dot{Q}_{II} + \dot{Q}_{III} + \dot{Q}_{IV} \tag{53}$$

$$A_{cc} = A_I + A_{II} + A_{III} + A_{IV} \tag{54}$$

2.7 Zone overall heat transfer coefficient and pressure drop

The overall heat transfer coefficient for zone, neglecting the thermal resistance due to heat conduction through the wall, is written in terms of the zone averaged heat transfer coefficients, α_j:

$$\frac{1}{U_i} = \sum_{j=1,2}\left(\frac{1}{\alpha_j}\right) \tag{55}$$

It is assumed that single-phase refrigerant pressure drop over each zone is due to frictional losses only.

$$\Delta P = \Delta P_f = 4\, f \frac{N_{cp}\, L_v}{D_h} \frac{G^2}{2\rho} \tag{56}$$

Where

$$G = \frac{\dot{m}}{N_{cp} b\, L_w} \tag{57}$$

$$D_h = \frac{2b}{\phi} \tag{58}$$

For two-phase refrigerant flow, pressure variation due to fluid acceleration is also included.

$$\Delta P = \Delta P_a + \Delta P_f \tag{59}$$

$$\Delta P_a = \left(\frac{G_{eq}^2\, x}{\rho_l - \rho_v}\right)_{out} - \left(\frac{G_{eq}^2\, x}{\rho_l - \rho_v}\right)_{in} \tag{60}$$

$$\Delta P_f = 4\, f \frac{N_{cp}\, L_v}{D_h} \frac{G_{eq}^2}{2\rho_l} \tag{61}$$

Where

$$G_{eq} = G\left[1 - x + x\left(\frac{\rho_l}{\rho_v}\right)^{1/2}\right] \tag{62}$$

2.8 Heat transfer coefficient and friction factor

Reviews on the heat transfer and pressure drop for single-phase, condensing and evaporating flows across plate heat exchangers can be found in the literature (e.g., Ayub, 2003; Khan and Chyu, 2010). They provide an overview of the available heat transfer and pressure drop correlations for specific geometries, fluids and experimental ranges of operation. For the purpose of the present paper, taking the average value over the zone area, the correlations of Kim (1999), Khan and Chyu (2010) and Han et al. (2003a, 2003b) were employed, for single-phase, evaporating and condensing flows, respectively. They are briefly described below.

2.8.1 Single-phase flow

Equations (63) to (65), from Kim (1999), were applied for all single-phase flows in the heat exchangers, including, vapour or liquid refrigerant and the condenser and evaporator heat transfer fluids.

$$\mathrm{Nu} = 0.295\ \mathrm{Re}^{0.64}\ \mathrm{Pr}^{0.32} \left(\frac{\pi}{2} - \beta\right)^{0.09} \tag{63}$$

Where

$$\mathrm{Nu} = \frac{\alpha D_h}{k} \tag{64}$$

$$\mathrm{Re} = \frac{G D_h}{\mu} \tag{65}$$

The single-phase Fanning friction factor is provided by Khan and Chyu (2010), for chevron angles of 30º and 60º.

$$f = C\,\mathrm{Re}^n \begin{cases} \beta = \pi/6: & C = 1.56; \quad n = -0.24 \\ \beta = \pi/3: & C = 34.43; \quad n = 0.5 \end{cases} \tag{66}$$

3. METHOD OF SOLUTION

Equations **Erro! Fonte de referência não encontrada.** to **Erro! Fonte de referência não encontrada.**, together with thermodynamic property equations, form a non-linear system of algebraic equations that has to be solved numerically. The Engineering Equation Solver platform, with built-in thermophysical properties calculation, was employed for the numerical solution. For the purposes of the present study the computational code was organized to provide system thermodynamic performance (mass flow rates and thermodynamic states of refrigerant and LTC and HTC heat transfer fluids) and sizing of components (heat transfer areas of all heat exchange control volumes and compressors displacements) from the following prescribed values: condensing and evaporating temperatures $\left(T_{ev,LTC}, T_{cd,LTC}, T_{ev,HTC}, T_{cd,HTC}\right)$, degrees of subcooling and superheating $\left(\Delta T_{sh,LTC}, \Delta T_{sc,LTC}, \Delta T_{sh,HTC}, \Delta T_{sc,HTC}\right)$, refrigeration load $\left(\dot{Q}_{ev}\right)$, heat transfer fluids inlet temperatures $\left(T_{sf,in}, T_{co,in}\right)$ and temperature differences across the evaporator and condenser $\left(\Delta T_{sf}, \Delta T_{co}\right)$. Further input values include a reference mass flux for each heat exchanger $\left(G_{cd}, G_{ev}, G_{cc}\right)$ and heat exchanger geometry parameters $\left(b, \phi, \beta, \lambda, p_{co}\right)$.

Having in mind that the numerical solution seeks the sizing of the heat exchangers and compressors, the computer program was organized in five major groups, as follows: (i) construction, from the input data, of a simplified reference cascade system, to serve as a guess solution; (ii) calculation of thermodynamic cycle from mass and energy conservation equations; (iii) calculation of heat conductances of each heat exchanger control volume, by the application of heat transfer and effectiveness equations; (iv) calculation of friction factor and heat transfer coefficient for each zone; (v) calculation of the areas and pressure drop for each zone. Groups (i) to (v) are not performed independently, or in sequence, as some variables depend on results from previous groups. For example, the boiling heat transfer coefficient, calculated in (iv), is dependent on the heat flux, i.e., the boiling zone heat transfer rate, (ii), divided by the heat transfer area, (v). Also, the pressure drop over each heat exchanger zone affects the entire system calculation and is, at the same time, dependent on the resulting heat exchanger geometry.

4. RESULTS

4.1 Comparison with Experimental Results

A simplified version of the computer programme (thermodynamic model, groups (i) and (ii)) was set to predict the performance of a NH_3/CO_2 cascade refrigeration system as tested by Bingming et al. (2009). Predicted values of the coefficient of performance, $COP = \dot{Q}_{ev} \Big/ \left(\dot{W}_{cpl} + \dot{W}_{cph}\right)$, were compared with experimental data made available in Bingming et al. (2009). Nineteen runs in total were compared, Fig. 3. It can be seen that agreement was reasonable, with the exception of one single point. It is not clear whether this larger discrepancy can be attributed to a measurement or simulation error or if the cascade-condenser approach of this run, coincidentally, the largest value in the set of points, has had some influence on this discrepancy. It should be emphasized, though, that this comparison only confirms the thermodynamic model (refrigerant energy balances, compressor and thermodynamic property equations), since Bingming et al. (2009) used shell-and-tube heat exchangers, leaving out verification of the heat transfer rate equations and the calculation of heat transfer areas.

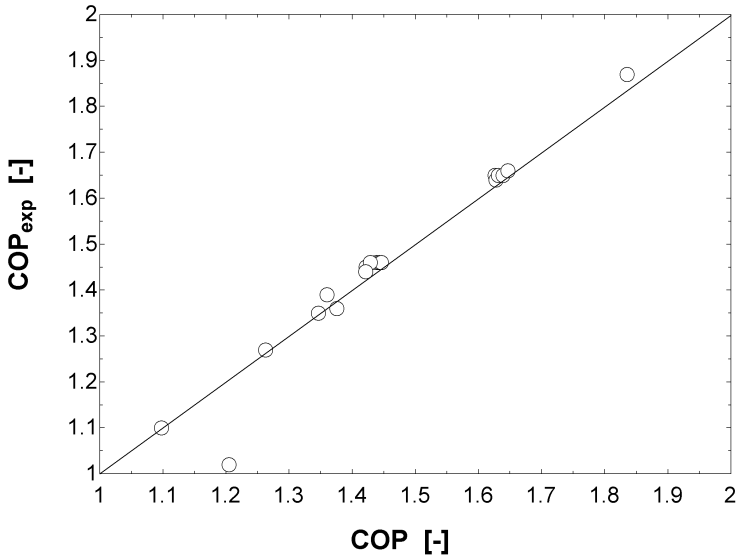

Figure 3 Comparison between predicted and experimental values of COP. Experimental data from Bingming et al. (2009): $T_{cd,HTC} = 40\,^{\circ}\mathrm{C}$ *;* $-23\,^{\circ}\mathrm{C} \le T_{ev,HTC} \le -5\,^{\circ}\mathrm{C}$ *;* $0\,^{\circ}\mathrm{C} \le \Delta T_{sh,HTC} \le 2\,^{\circ}\mathrm{C}$ *;* $\Delta T_{sc,HTC} = 5\,^{\circ}\mathrm{C}$ *;* $-20\,^{\circ}\mathrm{C} \le T_{cd,LTC} \le 0\,^{\circ}\mathrm{C}$ *;* $-50\,^{\circ}\mathrm{C} \le T_{ev,LTC} \le -35\,^{\circ}\mathrm{C}$ *;* $10\,^{\circ}\mathrm{C} \le \Delta T_{sh,LTC} \le 20\,^{\circ}\mathrm{C}$ *;* $\Delta T_{sc,LTC} = 0\,^{\circ}\mathrm{C}$.

4.2 Comparative study of refrigerants pairs

A preliminary simulation was carried out to investigate the performance of a cascade refrigeration system operating under typical conditions for a combination of refrigerant couples: R717, R404A and R407C, for the high temperature circuit, and R410A and R744, for low temperature. Table 1 depicts, for each refrigerant combination, the system coefficient of performance, the refrigerant mass flow rate ratio, $X_m = \dot{m}_{rf,HTC} / \dot{m}_{rf,LTC}$, refrigerant pressure drops and areas of the heat exchangers, the latter two relative to the values obtained for the NH_3-CO_2 pair. Greater COP values were obtained with CO_2 as the LTC refrigerant, if compared to R410A. Among the three options for the HTC refrigerant, refrigerant R404A presented the highest mass flow rate ratio and R717, the lowest, with trends in agreement with Bansal and Jain (2007). The NH_3-CO_2 combination also presented the lowest pressure drop and heat transfer area. However, care should be taken when extrapolating these findings to other conditions. Indeed, for a given set of heat source and heat sink temperatures, which, to a certain extent, define $T_{cd,HTC}$ and $T_{ev,LTC}$, still a number of degrees of freedom remain, including thermodynamic parameters, $T_{cd,LTC}$ and $T_{ev,HTC}$ (or ΔT_{cc}), $\Delta T_{sc,HTC}$, $\Delta T_{sh,HTC}$, $\Delta T_{sc,LTC}$ and $\Delta T_{sh,LTC}$, geometric, b, β, ϕ, λ and p_{co}, and operational, G, the latter two groups directly affecting the heat exchangers pressure drop, and, consequently, the cycle thermodynamic performance.

Table 1. Performance prediction of a cascade system operating with different pairs of refrigerants. Operating conditions: $\dot{Q}_{ev} = 10\,kW$; $T_{cd,HTC} = 40\,^{\circ}\mathrm{C}$; $T_{ev,HTC} = 2.5\,^{\circ}\mathrm{C}$; $\Delta T_{sh,HTC} = 10\,^{\circ}\mathrm{C}$; $\Delta T_{sc,HTC} = 10\,^{\circ}\mathrm{C}$; $T_{cd,LTC} = 7.5\,^{\circ}\mathrm{C}$; $T_{ev,LTC} = -30\,^{\circ}\mathrm{C}$; $\Delta T_{sh,LTC} = 10\,^{\circ}\mathrm{C}$; $\Delta T_{sc,LTC} = 10\,^{\circ}\mathrm{C}$; $G = 10\,kg\,s^{-1}m^{-2}$

LTC refrigerant HTC refrigerant	R744 R717	R744 R404A	R744 R407C	R410A R717	R410A R404A	R410A R407C
COP [-]	1.749	1.704	1.69	1.542	1.498	1.486
X_m **[-]**	0.289	2.529	1.873	0.264	2.314	1.713
$\frac{\Delta P_{ev}}{\Delta P_{ev,NH_3-CO_2}}$ **[-]**	1	1	1	5.74	5.74	5.74
$\frac{\Delta P_{cd}}{\Delta P_{cd,NH_3-CO_2}}$ **[-]**	1	1.62	1.61	1.05	1.70	1.70
$\frac{\Delta P_{cc,LTC}}{\Delta P_{cc,LTC,NH_3-CO_2}}$ **[-]**	1	1	1	2.56	2.56	2.56

$\frac{\Delta P_{cc,HTC}}{\Delta P_{cc,HTC,NH_3-CO_2}}$ [-]	1	2.42	2.39	1.09	2.97	2.91
$\frac{A_{ev}}{A_{ev,NH_3-CO_2}}$ [-]	1	1	1	1.49	1.49	1.49
$\frac{A_{cd}}{A_{cd,NH_3-CO_2}}$ [-]	1	2.91	3.99	1.05	3.05	4.17
$\frac{A_{cc}}{A_{cc,NH_3-CO_2}}$ [-]	1	1.99	1.86	1.08	1.76	1.50

5. CONCLUSIONS

A simulation model for two-circuit cascade refrigeration systems was developed. The performance of cascade systems is influenced by a significant number of parameters, suggesting the existence of an optimal combination of operational settings. In such a context, a simulation model may prove to be a valuable design tool. The present model adopted the lumped-parameter multi-zone method, which combines simplicity to computational speed. It goes beyond the simple thermodynamic analysis of the cycle, as it allows for the calculation of heat exchanger areas and a clear identification of single or two-phase areas within the three heat exchangers. Besides, should a more complex, elemental analysis be adopted, the control volume boundaries dictated by the present model can be advantageously used to define precise element limits, thus improving numerical efficiency.

6. REFERENCES

Ayub, Z. H., 2003, Plate heat exchanger literature survey and new heat transfer and pressure drop correlations for refrigerant evaporators, Heat Transfer Engineering, 24(5):3-16.

Bansal, P.K., Jain, S., 2007. Cascade systems: past, present and future, ASHRAE Trans, vol 11, I, 245-252.

Bhattacharyya, S., Mukhopadhyay, S., Sarkar, J., 2008. CO2-C3H8 cascade refrigeration-heat pump system: heat exchanger inventory optimization and its numerical verification, Int. J. Refrigeration, vol 31, pp. 1207-1213.

Bingming, W., Huagen, W., Jianfeng, L., Ziwen, X., 2009. Experimental investigation on the performance of NH3/CO2 cascade refrigeration system with twin-screw compressor, Int. J. Refrigeration, 32:1358-1365.

Brown, J. S., Yana-Motta, S.F., Domanski, P.A., 2002. Comparative analysis of automotive air conditioning systems operating with CO2 and R134a, , Int. J. Refrigeration, vol 25, pp. 19-32.

Di Nicola, G., Polonara, F., Sitryjek, R., Arteconi, A., 2011. Performance of cascade cycles working with blends CO2 + natural refrigerants, Int. J. Refrigeration, vol. 34, pp. 1436-1445.

Dopazo, J. A., Fernández-Seara, J., 2011. Experimental evaluation of a cascade refrigeration system prototype with CO2 and NH3 for freezing process applications, Int. J. Refrigeration, vol. 34, pp. 257-267.

Dopazo, J.A., Fernández-Seara, J., Sieres, J., Uhía, F.J., 2009. Theoretical analysis of a CO2-NH3 cascade refrigeration system for cooling applications at low temperature, Applied Thermal Engineering, 29:1577-1583.

Getu, H.M., bha, P.K., 2008. Thermodynamic analysis of an R744-R717 cascade refrigeration system, Int. J. Refrigeration, 31:45-54.

Han, D. H., Lee, K. J., Kim, Y. H., 2003a. Experiments on the characteristics of evaporation of R410A in brazed plate heat exchangers with different geometric configurations, Applied Thermal Engineering, 23(10):1209-1225.

Han, D. H., Lee, K. J., Kim, Y. H., 2003b. The characteristics of condensation in brazed plate heat exchangers with different chevron angles, Journal of the Korean Physical Society, 43(1):66-73.

Khan, M. S., Chyu, M. C. 2010, Evaporation in flooded corrugated plate heat exchangers with ammonia and ammonia/miscible oil, ASHRAE Technical Report RP-1352, Atlanta, GA, USA.

Kilicarslan, A., Hosoz, M., 2010. Energy and irreversibility analysis of a cascade refrigeration system for various refrigerant couples, Energy Conversion and Management, 51:2947-2954.

Kim, Y.S., 1999. An experimental study on evaporation heat transfer characteristics and pressure drop in plate heat exchanger, M.S. Thesis, Yonsei University, South Korea.

Le, C.V., Bansal, P.K., Tedford, J.D., 2004. Three-zone system simulation model of a multiple-chiller plant, Applied Thermal Engineering, 24, 1995-2015.

Lee, T., Liu C., Chen, T., 2006. Thermodynamic analysis of optimal condensing temperature of cascade-condenser in CO2/NH3 cascade refrigeration systems, Int. J. Refrigeration, 30:1100-1108.

Martins Costa, M. L., Parise, J. A. R., 1993. A three-zone simulation model for air cooled condensers, International Journal of Heat Recovery Systems & CHP, vol. 13, no. 2, pp. 97-113.

Messineo, A., Panno, G., 2011a. Thermodynamic analysis of a R744-R717 cascade refrigeration system compared with a R404A two-stage system, International Conference on Refrigeration, August 21-26, Prague, Czech Republic, paper 110.

Messineo, A., Panno, G., 2011b. Thermodynamic analysis of cascade refrigeration systems working with synthetic and natural refrigerants, International Conference on Refrigeration, August 21-26, Prague, Czech Republic, paper 128.
Pearson, S. F., 1999. Ammonia Refrigeration Systems, ASHRAE Journal, March, pp. 24-28.
Poggi, F., Macchi-Tejeda, H., Leducq, D., Bontemps, A., 2008. Refrigerant charge in refrigeration systems and strategies of charge reduction, Int. J. Refrigeration, 31, 353-370.
Rezayan, O., Behbahaninia, A., 2011. Thermoeconomic optimization and exergy analysis of CO2/NH3 cascade refrigeration systems, Energy, 36, 888-895.
Sawalha, S., 2005. Using CO2 in supermarket refrigeration, ASHRAE Journal, vol. 47, no. 8, pp. 26-30.